ACS Catalysis

Research Article

pubs.acs.org/acscatalysis

In Situ X-ray Absorption Spectroscopic Analysis of Gold−Palladium Bimetallic Nanoparticle Catalysts

Aimee Maclennan,[†] Abhinandan Banerjee,[†] Yongfeng Hu,[‡] Jeffrey T. Miller,[§] and Robert W. J. Scott*[,†]

[†]Department of Chemistry, University of Saskatchewan, 110 Science Place, Saskatoon, SK S7N 5C9, Canada

[‡]Canadian Light Source, University of Saskatchewan, Saskatoon, SK S7N 0X4, Canada

[§]Chemical Sciences and Engineering Division, Argonne National Laboratory, Argonne, Illinois 60439-4837, United States

ABSTRACT: Gold−palladium core−shell nanoparticles have been previously shown to be extremely effective catalysts for a number of oxidation reactions including the aerobic oxidation of alcohols. However, the novel activity and durability of such catalysts are still poorly understood, and there are several putative mechanisms by which oxidation reactions can proceed. Previously we showed that Pd(II) salts in the presence of Au nanoparticles were also effective catalysts for the room temperature oxidation of crotyl alcohol. Herein we show an in situ X-ray absorption spectroscopy (XAS) study at both the Pd−K and Pd-L_{III} edges of Au nanoparticle/Pd(II) salt solutions in the presence of crotyl alcohol. Liquid cells with X-ray permeable windows were used to obtain quick-scan XAS data during the oxidation of crotyl alcohol, allowing for time-resolved Pd speciation information and information about the reaction mechanism and kinetics. XAS measurements definitively show that the first step of this reaction involves Pd reduction onto the Au nanoparticles; in addition, further studies of the stability of the resulting Au−Pd core−shell nanoparticles toward oxygen gas suggests that the role of Au in such catalysts is to prevent the reoxidation of the catalytically active surface Pd atoms. Catalytic crotyl alcohol oxidation measurements were done which validated that the in situ reduction of Pd(II) in the presence of Au nanoparticles did indeed result in catalytically active AuPd bimetallic catalysts.

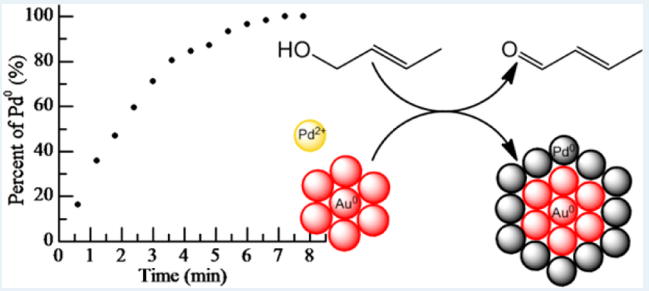

KEYWORDS: *alcohol oxidation catalysis, gold-palladium nanoparticles, X-ray absorption spectroscopy, in situ study, nanocatalysis*

1. INTRODUCTION

The extensive and ongoing study of nanoparticle catalysts began when it was first discovered that metal particles less than 10 nm in diameter behaved much differently than their bulk counterparts.[1] Small nanoparticles (NPs), because they possess a large amount of surface area, are often more catalytically active than the bulk material.[1−4] Au is one of the most commonly studied nanoparticle catalyst materials, and it is used in reactions such as CO and alcohol oxidations, dehydrogenations, and olefin hydrogenation reactions.[5,6] In recent years it has been discovered that the size, morphology, and characteristics of Au NPs can be tuned by synthesizing Au NPs with different stabilizers and/or placing them on a variety of supports.[2,5,7−10] The catalytic activity of nanoparticle catalysts can also be tuned by mixing Au with other metals such as Pt, Ag, Cu, and Pd.[9−21] In particular, mixing Au with Pd has led to substantially more efficient catalysts for a number of oxidation reactions. For example, AuPd catalysts have recently been used extensively for selective oxidation reactions of both alcohols and toluene as well as the direct formation of hydrogen peroxide from hydrogen and oxygen.[4−6,9,10,17]

The oxidation of alcohols is important in many pharmaceutical and industrial processes.[6,22] The AuPd nanoparticle-catalyzed oxidation of both saturated and $\alpha-\beta$ unsaturated alcohols has been studied in detail by both ourselves[23,24] and a number of other research groups.[9,25−38] However, the definitive mechanism by which the reaction takes place remains unclear at this time. Two proposed mechanisms which have received experimental support for the oxidation of $\alpha-\beta$ unsaturated alcohols include β-hydride (β-H) elimination over a zerovalent surface[3,23,24,39] or a redox mechanism involving Pd(II) formation and rereduction,[24] which are both shown in Scheme 1. β-H elimination occurs by the binding of the alcohol substrate to the nanoparticle surface, where it undergoes a β-H elimination reaction. Upon completion of the alcohol oxidation the product is removed from the NP surface leaving adsorbed hydrogen on the nanoparticle surface. At this point, molecular oxygen is required to strip the hydrogen from the nanoparticle surface (Scheme 1A). Support for this mechanism includes the identification of hydrogenation and isomerization side-products during crotyl alcohol oxidations over AuPd catalysts,[23,24] although there is evidence that this occurs only in the early stages of the reaction. For the redox mechanism, Pd from the surface of the bimetallic nanoparticle becomes oxidized, followed by the stoichiometric reaction of the oxidized Pd species and the alcohol, upon which the Pd becomes reduced

Received: November 15, 2012
Revised: May 7, 2013
Published: May 14, 2013

   dx.doi.org/10.1021/cs400230t | ACS Catal. 2013, 3, 1411−1419

Scheme 1. Suggested Mechanisms for the Oxidation of Crotyl Alcohol over AuPd Nanoparticles in the Presence of O_2: (A) β-H Elimination Mechanism, (B) Redox Mechanism

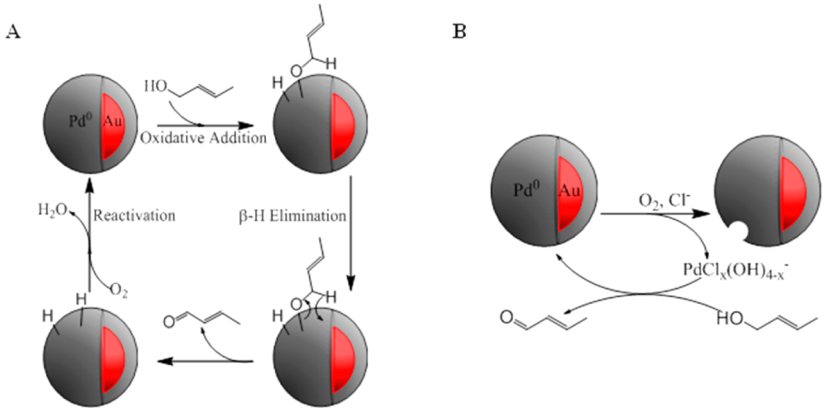

and alcohol is oxidized (Scheme 1B). We previously saw some evidence for this mechanism when we carried out the oxidation of crotyl alcohol in the presence of Au NPs and K_2PdCl_4. Upon introduction of crotyl alcohol into the Au NP/Pd(II) mixture at room temperature, the NPs significantly grew in size, suggesting Pd(II) reduction onto the Au NPs.[24] This was confirmed by ex situ EXAFS analysis of the catalysts after the oxidation reaction. This result is similar to that seen by Lee and co-workers in which PdO was found to reduce to Pd in the presence of cinnamyl alcohol by XAS.[40] Prati and co-workers showed that monometallic Au and Pd NPs form AuPd catalytic NPs in situ, which supports a redox mechanism.[33] In addition, Lee and co-workers have shown that PdO species on the surface of Pd particles are the catalytic species via in situ X-ray absorption spectroscopy and XPS studies of gas-phase oxidations of allylic alcohols at temperatures between 60 and 250 °C.[27,30,34,40]

To gain insight into the mechanism of the oxidation of $\alpha-\beta$ unsaturated alcohols, a series of reactions were carried out, and the effects of Pd in the system were studied in situ by X-ray absorption spectroscopy (XAS). XAS analysis is used to determine characteristics such as oxidation state, coordination number, and bond lengths of a material,[10,41−45] and is traditionally performed on a solid sample. With recent advances in XAS technology it has now become possible to analyze materials under reactive conditions, including samples under in situ conditions in both the solid and the liquid phase and the ability to study reaction kinetics with fast scans.[34,46] To perform such analyses the experimental set up requires new and innovative designs of sample cells. Liquid and solid cell designs have been fabricated such that samples can be heated and exposed to different atmospheric environments.[46] Such capabilities allow for in situ and/or in operando verification of the oxidation states and coordination environments of transition metal catalysts. For example, Ishiguro et al. and Imai et al. have used in situ time-resolved XAFS to study platinum cathode catalysts in polymer electrolyte fuel cells,[47−49] and Lee and co-workers have shown PdO formation during the aerobic oxidation of alcohols over Pd NP catalysts.[27,30,34,40]

In this study, we have used in situ X-ray absorption spectroscopy to follow the Pd(II)/Au nanoparticle catalyzed oxidation of crotyl alcohol in aqueous solutions. Significantly, both Pd−K edge and lower energy Pd-L_{III} edge in situ studies were carried out to examine Pd speciation upon introduction to crotyl alcohol substrates and oxygen gas. Results show that in the initial stages of this reaction, K_2PdCl_4 salts are reduced on the Au nanoparticle surface, and the kinetics of this reduction have been analyzed. Pd L_{III} edge spectra after reduction suggest the bimetallic NPs are slightly electron-deficient compared to their pure Pd nanoparticle counterparts. In addition, the final AuPd catalysts were found to be exceptionally stable to oxygen once formed, thus suggesting that a Pd redox mechanism will not proceed to a significant extent after initial catalyst formation. Thus these in situ X-ray absorption spectroscopy measurements allow valuable information as to the plausible catalytic pathways under appropriate reaction conditions.

2. EXPERIMENTAL SECTION

2.1. Materials. The following chemicals were purchased from Alfa Aesar and used as received: Polyvinylpyrrolidone (PVP) MW 58,000 g/mol, sodium borohydride ($NaBH_4$, 98%), ascorbic acid (99%), tetrachloroauric acid ($HAuCl_4{\cdot}3H_2O$, 99.99%), potassium tetrachloropalladate (K_2PdCl_4, 99.99%), and 2-buten-1-ol (crotyl alcohol, 96%). 18MΩ cm Milli-Q water (Millipore, Bedford, MA) was used throughout.

2.2. Synthesis of PVP Stabilized Pd, Au, and AuPd NPs in Water. PVP-stabilized monometallic Au and Pd nanoparticles, as well as sequentially reduced bimetallic AuPd nanoparticles were synthesized by previously reported procedures;[23,24,50] monometallic NPs were synthesized using sodium borohydride as a reducing agent, while the sequentially reduced NPs were synthesized by selectively reducing a Pd shell onto Au "core" NP seeds using ascorbic acid.

Synthesis of monometallic Au NPs (also used as "seed" particles in the synthesis of bimetallic NPs) was carried out by mixing 6.30 mL of 10 mM $HAuCl_4$ $3H_2O$ (6.30×10^{-5} mol) with 25 mL of 0.88 mM PVP (2.2×10^{-5} mol) and allowing the mixture to stir at 800 rpm for 30 min at room temperature, under N_2. The mixture was then placed on ice, and 6.30 mL of 100 mM $NaBH_4$ (6.30×10^{-4} mol) was added quickly to the solution, stirring at 1200 rpm. The reduced NPs were allowed to stir for 30 min on ice, then an additional 30 min at room temperature. The reaction was quenched by adding 6.30 mL of 100 mM HCl (6.30×10^{-4} mol), and stirring for 30 min. An additional 20 mL of 1.5 mM PVP (3.0×10^{-5} mol) was added to the NP solution to further stabilize the particles. The particles were then dialyzed overnight in 1 L of water (changed 4 times) using cellulose dialysis membranes with a molecular cut off of 124,000 g/mol, under N_2. The dialyzed NPs (ca. 1 mM in terms of metal concentration) were then concentrated

dx.doi.org/10.1021/cs400230t | ACS Catal. 2013, 3, 1411−1419

under vacuum at 25 °C to obtain a final Au concentration of 3.13 mM. Monometallic Pd NPs were synthesized in the same manner as the Au NPs, using K_2PdCl_4 instead of $HAuCl_4{\cdot}3H_2O$. The Pd NPs were concentrated to 9.44 mM, rather than the 3.13 mM of the Au NPs.

Sequentially reduced NPs were synthesized by mixing 33.11 mL of previously prepared (as aforementioned) 1 mM PVP-stabilized Au NPs (3.13×10^{-5} mol Au) with 4.7 mL of 200 mM ascorbic acid (9.4×10^{-4} mol) and placing the mixture in an ice bath, under N_2. To this mixture, 4.7 mL of 20 mM K_2PdCl_4 was added, and the solution was stirred at 1200 rpm for 1 h. Ascorbic acid is used in this step for the controlled reduction of Pd(II) onto the Au NP surface. The sequentially reduced NPs were then dialyzed overnight in the same manner as the monometallic NPs. The bimetallic NPs were then concentrated under vacuum at 25 °C to achieve final concentrations of 3.13 mM and 9.44 mM in terms of Au and Pd, respectively

2.3. Characterization. Transmission electron microscopy (TEM) analyses of the NPs were conducted using a Philips 410 microscope operating at 100 kV. The samples were prepared by drop-casting a small amount of dilute, aqueous sample onto a plasma cleaned carbon-coated copper TEM grid (Electron Microscopy Sciences, Hatfield, PA). Average particle diameters were determined by manually measuring 200 NPs from each sample using the ImageJ program.[51]

Pd K edge and Au-L_{III} edge X-ray absorption measurements were conducted on the insertion device beamline of the Materials Research Collaborative Access Team (MRCAT, 10-ID) at the Advanced Photon Source (APS) in Argonne, IL. Full EXAFS measurements were done before and after in situ measurements using an energy scan range for the Au-L_{III}-edge of 11,700 to 12,800 eV and an energy scan range for the Pd−K-edge of 24,050 to 25,400 eV while fast XANES measurements of the Pd edge up to k = 8 were made every 0.6 s. The X-ray measurements were conducted in ion chambers filled with a helium and nitrogen mixture for the Pd−K-edge measurements. Pd and Au foils were used for the respective edges as references. All XAFS measurements were conducted in fluorescence mode.

The Sector 9-BM beamline at the APS was used to collect XANES spectra at the Pd-L_{III} edge from 3,140 eV to 3,225 eV. The X-ray measurements were conducted in using helium as the inert atmosphere. In situ measurements were taken at this same range and scans were performed every 9.5 min. Photoreduction of Pd on the Pd-L_{III} edge was problematic for aqueous solutions of Pd(II) salts at high beam fluxes; care was taken to lower the beam flux by defocusing and/or filtering the beam with Kapton filters and stir the sample via magnetic stirring such that that photoreduction events were not occurring in the experiments. Such photoreduction effects were not seen at the higher energy Pd K-edge, likely because of the much greater transparency of water at this energy.

The IFEFFIT software package was used for XAFS data processing, and the spectra were analyzed using methods previously stated.[52−54] The background in each postedge was fit to a cubic spline function while the pre-edge region was fit with a straight line. The EXAFS function, χ, was obtained by subtracting the postedge background from the overall absorption and then normalizing with respect to the edge jump step. The EXAFS fitting was performed in R-space for the Au and Pd edges. A theoretical AuPd alloy model was constructed based on a AuPd lattice parameters and used for fitting.[55] fcc bulk lattice parameters (i.e., first shell coordination numbers of 12) were used to determine the amplitude reduction factor, S_0^2, for Au and Pd by analyzing Au and Pd reference foils.

2.4. General Procedure for in Situ Reactions. In situ reactions were carried out at the aforementioned beamlines, each beamline employing a different type of liquid cell. The liquid cell used at the 10-ID beamline was fabricated out of polyether ether ketone (PEEK), with Kapton windows on the side of the cell.[46] The liquid cells used for XANES analysis at the 9-BM beamline were SPEX CertiPrep Disposable XRF X-Cell sample cups with 4 μm Ultralene window film (purchased from Fisher Scientific, Ottawa, ON). Deionized water was used as the liquid medium throughout.

In situ reactions were performed by transferring a determined amount of Au "seed" NPs to the liquid cell then weighing a desired amount of K_2PdCl_4 ("Pd Salt"), suspending it in a minimal amount of water, and transferring to the Au seeds via pipet. To the Au NP/Pd Salt solution, a determined amount of crotyl alcohol ("substrate") was added via syringe. The mixture was quickly shaken by hand and stirred open to air with a magnet stir bar during XAFS measurements. Au and Pd foils, as well as 10 mM solutions of $HAuCl_4$ $3H_2O$ and K_2PdCl_4 were used as references. During experiments where oxygen was required, a 20% mix of O_2 in He was used.

2.5. General Procedure for Ex Situ Crotyl Alcohol Oxidation Reactions. Ex situ catalytic experiments were done at the same PVP-stabilized Au NPs and K_2PdCl_4 concentrations that were used for the 1:3 Au:Pd(II) in situ reactions. A 5.0 mL aqueous solution of Au NPs and K_2PdCl_4 ([Au] = 3.13 mM, [Pd] = 9.36 mM) was used for each experiment. Three experiments were run; Reaction A consisted of adding 93.6 μmol (10 μL) of crotyl alcohol (2 equiv based on Pd) to the 1:3 Au:Pd(II) solution under 1 atm of N_2 at 21 °C. After 1 h, the reaction was stopped, and the products were extracted three times with ethyl acetate and analyzed by GC. Reaction B was set up identically to Reaction A under N_2, except after 1 h, an additional 248 equiv (11.6 mmol, 1.044 mL) of crotyl alcohol was added to give a total Pd:substrate ratio of 1:250. The reaction mixture was flushed with 1 atm O_2 gas for several minutes. After this, the reaction was left under 1 atm of O_2 gas for 3 h at 21 °C, then the reaction was stopped and product extracted as described above. Finally, Reaction C was set up with a 1:3 Au:Pd(II) solution under 1 atm of O_2, followed by the addition of 250 equiv of crotyl alcohol (based on Pd; 11.7 mmol, 1.053 mL), followed by reaction for 3 h at 21 °C; the reaction was sampled at hourly intervals. Conversion, selectivity, and turnover numbers for the reactions were obtained from GC using a FID detector (Agilent Technologies 7890A) and a HP-Innowax capillary column used similar to previous work.[24] Turnover numbers (TONs) were calculated as moles products/mol total metal catalyst (such that they were consistent with previous work); turnover frequencies were determined by linear fits of plots of TONs vs time.

3. RESULTS AND DISCUSSION

3.1. Nanoparticles Synthesized for Quantitative Analysis of Crotyl Alcohol Oxidation versus Those Used for XAFS Analysis. The preparation of monometallic and sequentially reduced NPs for liquid XAFS measurements is carried out in the same manner as those prepared for use in the quantitative analysis of the NP-catalyzed oxidation of crotyl alcohol as described previously.[23,24] However, the concen-

dx.doi.org/10.1021/cs400230t | ACS Catal. 2013, 3, 1411−1419

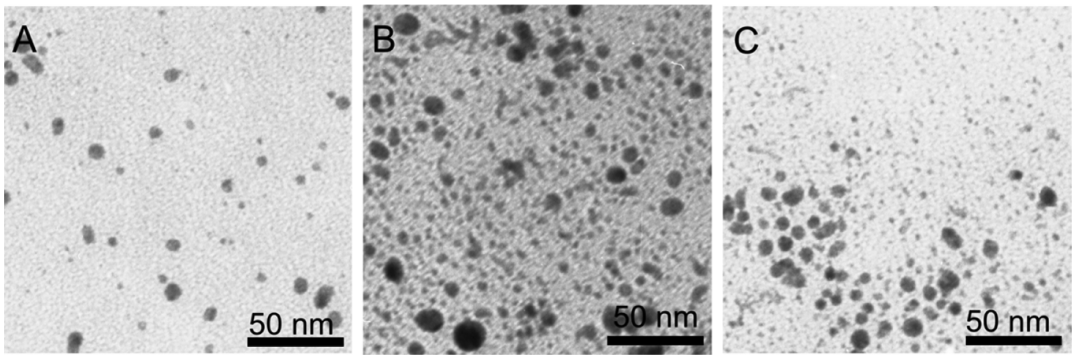

Figure 1. TEM images of concentrated PVP-stabilized (A) Au nanoparticles, (B) Pd nanoparticles, and (C) sequentially reduced 1:3 Au core: Pd shell nanoparticles.

tration of metal needed for liquid XAFS measurements is approximately 20 times more concentrated than those used for catalytic studies of the quasi-homogeneous oxidation of crotyl alcohol using PVP-stabilized AuPd NPs. During the synthesis of NP samples for XAFS analysis, the NPs are concentrated under vacuum using moderate temperatures. This concentration step inevitably led to some sintering and thus a larger polydispersity in particle sizes. TEM images for Au, Pd, and sequentially reduced AuPd NPs synthesized for liquid XAFS measurements are shown in Figure 1, and a summary of NP sizes is given in Table 1. The average particle sizes of the final particles are in the 5−6 nm range with moderate polydispersity, which is larger than 3−5 nm particles used in previous catalytic studies. Nevertheless, since in this study we are not performing a quantitative catalytic analysis for the oxidation of crotyl alcohol but rather analyzing the changes in the NP surfaces during the reaction, the larger NPs still allow us to gain valuable information about this system.

Table 1. Summary of Nanoparticle Sizes

nanoparticle	nanoparticle diameter (nm)
Au	5.5 ± 2.5
Pd	5.8 ± 3.1
1:3 Seq. Grown AuPd	6.0 ± 3.1

3.2. In Situ XANES Analysis of Crotyl Alcohol Oxidation in Water. X-ray absorption near-edge spectroscopy (XANES) analysis was performed on the Pd-L_{III}-edge for a series of Au NPs/Pd salt (K_2PdCl_4) catalyzed oxidation reactions of crotyl alcohol. XANES analysis is often used to determine the oxidation states of metals, particularly at the surfaces of materials. The oxidation state of Pd is related to the intensity of the white line absorption peak, as well as the energy at which the absorption peak arises. The absorption peak arises from the excitation of electrons from the 2p core into unfilled 4d states.[56,57] As empty 4d states of the Pd in the system become occupied, or the Pd becomes reduced, a decrease in white line intensity will occur.[58] In addition, a shift in the absorption maximum is expected with Pd reduction. For in situ XANES analysis, linear combination analysis fitting was done using two standards which represented fully reduced and fully oxidized Pd. The standard used to determine Pd(II) was a 10 mM solution of the K_2PdCl_4 in water, while that for Pd(0) was a fully reduced sample of sequentially reduced 1:3 AuPd NPs. The standard spectras were used to calculate the extent of the reduction of Pd(II) in the system during in situ reactions.

To determine if the reduction of Pd onto the Au NP surface occurs spontaneously, or if a reductant is required, an initial XANES measurement of Au NPs in the presence of Pd salt was taken. The spectrum obtained for this mixture (not shown) produced an edge-jump with a large white line intensity which was identical in intensity to the pure K_2PdCl_4 salt solution, indicating that the Pd was still in the Pd(II) oxidation state and did not spontaneously reduce to Pd(0) in the presence of Au NPs. To this solution, crotyl alcohol substrate was added into the liquid cell to give a substrate: metal molar ratio of 250:1. Figure 2 shows the comparison of the Pd-L_{III}-edge XANES of

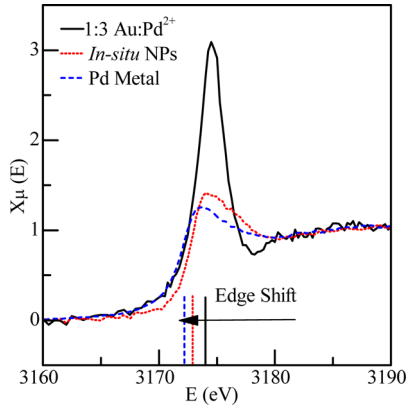

Figure 2. XANES Pd-L_{III} spectra comparing 1:3 Au:Pd^{2+} in water, NPs formed in situ after the addition of crotyl alcohol to 1:3 Au:Pd^{2+} in water in a 250:1 substrate:metal ratio, and pure Pd metal. The shifts in respective absorption edges are shown at the bottom of the spectra.

Au NPs and Pd(II) salt in solution before the addition of crotyl alcohol (black). The large excess of substrate caused the Pd(II) to reduce quickly, therefore the reaction was complete before the first XANES scan was completed (subsequent scans were identical to the first). The decrease in the amplitude of the edge jump after the addition of crotyl alcohol to the Au NP/Pd(II) salt mixture can be clearly seen in Figure 2. The absorption edge of each spectrum was also determined by taking the derivative of the spectrum. The absorption edges of each spectra are depicted at the bottom of Figure 2, showing that the edge shifts to lower energies from the Pd(II) starting material, to the final reduced sample formed in situ and to the metal foil. The edge shift to lower energies is also an indication of Pd reduction. As the empty d states are filled, the energy gap between the 2p and empty 4d state becomes smaller, therefore the energy required to excite a core electron from the 2p state

dx.doi.org/10.1021/cs400230t | ACS Catal. 2013, 3, 1411−1419

to another empty d state also becomes smaller.[59] The shift toward lower excitation energy between the before and after addition of crotyl alcohol to the Au NPs/Pd salt solution signifies that the Pd is reduced by the crotyl alcohol. However, it can be seen that the absorption energy of the AuPd NPs formed after the addition of crotyl alcohol is at a slightly higher energy than the metallic Pd foil. The difference in absorption energies may be due to an electronic effect occurring between the Au NPs and Pd Shell, in which electron density is drawn away from the Pd by Au, causing the absorption edge to occur at a slightly higher energy. Alternatively, it is also possible this shift is due to Cl^- absorption on the Pd surface. Thus the Pd L_{III} edge data is consistent with the reduction of Pd on the Au NP surfaces upon exposure to crotyl alcohol, but do not rule out the possibility of secondary Pd nucleation. This result is consistent with the observations of others who have shown stoichiometric reactions of Pd(II) salts with allylic alcohols, typically giving the aldehyde and a Pd metal precipitate after the reaction.[61] Later EXAFS studies are more definitive with regards to bimetallic AuPd NP formation.

3.3. In Situ XAS Analysis of Crotyl Alcohol Oxidation in Water. The reduction of Pd(II) onto Au NPs by the addition of crotyl alcohol was also studied in situ by Pd–K-edge XANES, an excitation of a core 1s electron to an unoccupied 4p state. Quick XAS scans of each sample were taken from 150 eV before the absorption edge to 445 eV (k = 8) after every 36 s. Time-resolved normalized XANES data in E space for the in situ reaction of 1:1 Au NPs:Pd(II) and 1:1/2 Pd:substrate ratios is shown in Figure 3. Time-resolved spectra in E space (Figure 3A) clearly shows spectral changes with reaction progress. As the reaction proceeds the first feature after the absorbance edge (labeled A) slowly transforms into two narrow peaks. Comparison to references confirms that this spectral change corresponds to the Pd(II) in solution being reduced to Pd(0) upon the addition of crotyl alcohol. Small changes in further XANES features (B–D) can also be seen as the reaction progresses. The same data set is also shown in R-space in Figure 3B. Two significant features in this spectrum are seen which correlate to the Pd–Cl bond and the Pd–M bond, a mixture of Pd–Pd and Pd–Au bonding. As the reaction progresses the Pd–Cl peak decreases in amplitude while the Pd–M feature increases. Because the Pd–Cl peak decreases as the Pd–M increases it can be said that Pd(II) is indeed being reduced. Linear combination analysis was also performed on the E space data for this reaction from 30 eV before to 30 eV after the edge. Reference spectra used were K_2PdCl_4 mixed with Au NPs and a fully reduced, presynthesized sample of AuPd NPs. The Pd–K-edge XANES were fit with a linear combination of that for K_2PdCl_4 and fully reduced AuPd NPs and is shown in Figure 4. The reduction of Pd(II) occurs quickly for about 4 min, then begins to plateau, and after 8 min the Pd is fully reduced. Kinetic treatment of the data indicates that the reduction of Pd(II) onto the Au surface is a first order reaction with a rate constant of 0.0468 min^{-1}.

3.4. Oxidation of Nanoparticles. According to the redox mechanism for the oxidation of crotyl alcohol, the presence of molecular oxygen is required to oxidize Pd(0) from the surface of the nanoparticle, forming a catalytically active Pd(II) species either in solution or on the surface of the nanoparticle. If the reaction proceeds by this mechanism, a sample of AuPd NPs which has been exposed to oxygen for long time periods should show signs of oxidation. A sample of the nanoparticles formed in situ during the reaction of 1:1 Au NPs: Pd(II), and a 1:1

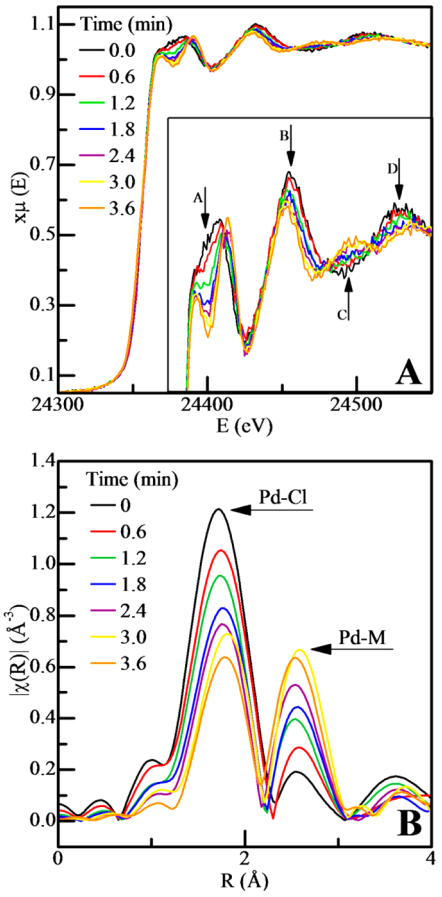

Figure 3. Time resolved Pd K-edge XAFS in (A) E-space with inset of enlarged postedge image and (B) R-space for the nanoparticles formed in situ during the oxidation of crotyl alcohol in water. Au:Pd = 1:1, Pd: Substrate = 1:1/2.

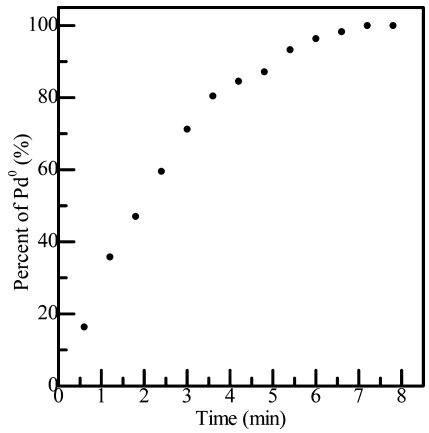

Figure 4. Linear combination of the Pd–K-Edge EXAFS spectra for the nanoparticles formed in situ during the oxidation of crotyl alcohol. Au:Pd = 1:1, Pd: Substrate = 1:1/2.

substrate to Pd ratio was treated with a mixture of 20% oxygen in helium for variable amounts of time. The spectra of the Pd-L_{III} edge in E space for each scan of the nanoparticles after oxygen treatment are shown in Figure 5. XANES analysis is more sensitive to changes in oxidation state than EXAFS, therefore we compared these spectra to determine if the NPs are easily oxidized. Only very minute changes can be seen in the spectra even after exposure to oxygen for 7 h. EXAFS fitting

dx.doi.org/10.1021/cs400230t | ACS Catal. 2013, 3, 1411–1419

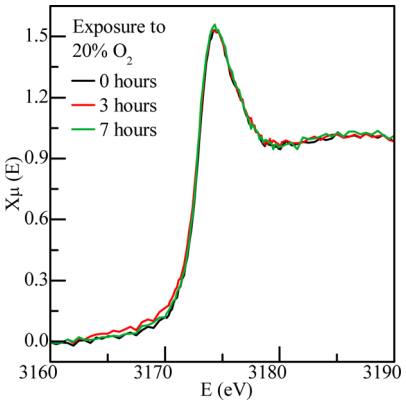

Figure 5. Pd-L_{III}-Edge in E-space for nanoparticles formed in situ which have subsequently been exposed to a 20% mixture of O_2 in He for varying amounts of time.

analysis was also performed on similarly collected Pd K-edge data, and a summary of the fitting results is shown in Table 2. It

Table 2. EXAFS Fitting of Nanoparticles Exposed to Oxygen for Varying Amounts of Time[a]

time exposed to 20% O_2 (min)	shell	N	R (Å)	ΔE_o (eV)	R-factor
0	Pd–Pd	6.8(0.2)	2.748(0.003)	−5.2(0.3)	0.003
	Pd–Au	2.8(0.3)	2.77(0.02)		
180	Pd–Pd	6.3(0.2)	2.745(0.004)	−4.9(0.4)	0.008
	Pd–Au	3.3(0.4)	2.76(0.02)		

[a]Values of σ^2 for the Pd–Pd and Pd–Au shells were fixed at 0.0079 Å^2 and 0.012 Å^2, respectively. A S_o^2 value of 0.93, determined from Pd foil, was used for Pd fitting.

can be seen that there are no significant changes in coordination number or bond distances, even after 3 h of oxygen treatment. Thus, both sets of data show that no significant Pd oxidation is occurring during treatment with molecular oxygen, thus it is unlikely the alcohol oxidation reaction proceeds via a redox mechanism at room temperature.

Others have shown that, upon exposure to allylic alcohols, Pd(II) does reduce into Pd black.[60,61] Small monometallic Pd NPs are very susceptible to oxidation;[62] thus if pure Pd NPs were formed by secondary nucleation in situ, we would expect a larger change in the Pd-L_{III}-edge upon exposure to oxygen. Since there is no significant change in the Pd-L_{III} edge spectra, or the Pd–K edge EXAFS fitting, the formation of small Pd NPs can likely be ruled out. Goodman and co-workers have also previously shown that Pd deposited onto Au is much less susceptible to oxidation.[63] It should be noted that there is a possibility that very low levels of Pd(II) are responsible for catalytic activity; as XANES is a bulk technique, ultralow levels of Pd(II) could be averaged out by bulk Pd(0) signal and thus be undetected. However, given that pure Pd particles have been shown to have much lower activity under such conditions than PdAu particles,[24] despite the fact that they are more susceptible to oxidation, we do not believe that a redox mechanism is at work.

3.5. Ex Situ Catalytic Oxidations of Crotyl Alcohol. Lee and co-workers have shown by in situ XAS spectroscopy that the active state for allylic alcohol oxidation over pure Pd nanoparticles is PdO, and not Pd metal.[27,40] Given these findings, we wanted to ensure that the surface Pd(0) which is formed in situ during the reactions above is in fact the active catalyst for crotyl alcohol oxidation; a second alternative explanation could be that Pd(0) formation was due to poisoning of the catalytic system as Pd(II) was converted to Pd(0). To rule out this second possibility, ex situ catalytic oxidation reactions were examined for this system. Three reactions were examined at room temperature (~21 °C) conditions, and the results are tabulated in Table 3. Reaction A

Table 3. Ex Situ Catalytic Results for the Oxidation of Crotyl Alcohol with 1:3 Au:Pd(II) Systems

reaction	catalyst system	time	conversion	selectivity to crotonaldehyde
A	Pd:substrate = **1:2** (under N_2)	1 h	48.8%	100%
B	sample A with new Pd:substrate = **1:250** (under O_2)	1 + 3 h[a] (4 h total)	74.5%	81.7%
C	Pd:substrate = **1:250** (under O_2)	1 h	20.6%	30.6%
		3 h	72.4%	62.8%

[a]An additional 248 equiv of crotyl alcohol was added to Reaction A after 1 h, and the system was saturated with 1 atm O_2(g).

involved the stoichiometric reaction of Pd(II) salts with crotyl alcohol under nitrogen conditions in the presence of the Au nanoparticles (with a Au:Pd(II) ratio of 1:3) and a 1:2 ratio of Pd:crotyl alcohol. A 48.8% conversion of crotyl alcohol was seen under these conditions to the single product crotonaldehyde after 1 h.[60,61] This represents a nearly stoichiometric reaction between Pd(II) and the substrate. After 1 h, an additional 248 equiv of crotyl alcohol were added to the mixture, and the atmosphere was switched to 1 atm O_2; and the reaction was continued for another 3 h. After 3 h, a total conversion of 74.5% of crotyl alcohol was observed, with an 81.7% selectivity to crotonaldehyde (reaction B; isomerization and hydrogenation products were also observed). This result suggests that the system was ***not*** poisoned by the initial Pd(II) reduction to form Pd(0) on the surface of the particles. Indeed, a third reaction (reaction C) in which a 1:250 Pd:crotyl alcohol ratio was present from the start of the reaction under oxygen gave comparable results to reaction B after 3 h (72.4% conversion), albeit with lower selectivities toward crotonaldehyde (62.8%). These results are consistent with our previous work,[24] and unambiguously show that Pd(0) formation is not leading to poisoning in this catalytic system; rather, the AuPd nanoparticles formed after Pd(II) reduction are in fact the active catalyst for this system. The turnover frequency (TOF) for reaction C over the first 2 h was 37 h^{-1}, which was slower than previous work with a similar Au NP/Pd(II) crotyl alcohol oxidation at lower metal concentrations (TOF ~ 68 h^{-1} over a similar time range).[24] The differences in kinetics are likely due to the much larger particle sizes seen in this study because of the higher concentrations used, and thus corresponding lower % of active Pd on the surface of the particles. The appearance of hydrogenation and isomerization products (1-butanol and but-3-ene-1-ol, respectively) during the reaction also supports β-hydride elimination mechanisms over a Pd(0) surface.[24] We are uncertain as to why selectivity data is improved for reaction B (in which Pd reduction occurred before catalysis), but do note that these results are in agreement with previous results in our group which showed that preformed AuPd core–shell particles

dx.doi.org/10.1021/cs400230t | ACS Catal. 2013, 3, 1411–1419

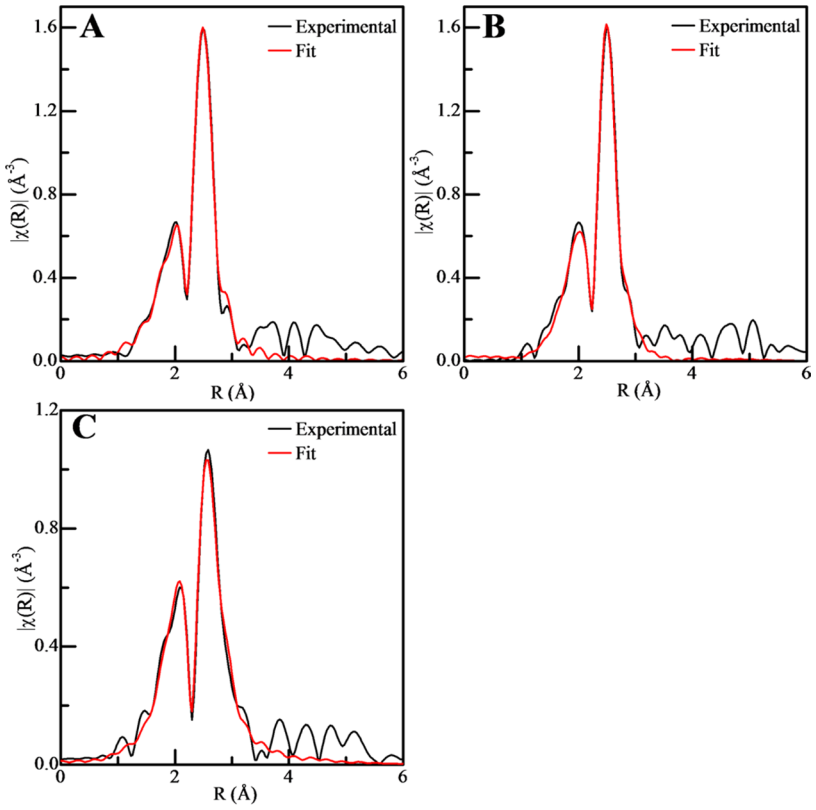

Figure 6. EXAFS spectra in R space and their respective fits to determine characteristics of the nanoparticles formed in situ for (A) 1:3 AuPd, 250:1 substrate:metal ratio, (B) 1:3 AuPd, 1:1 Pd:substrate, and (C) 1:1 AuPd, 1:1/2 Pd:substrate.

Table 4. Summary of EXAFS Fits[a]

nanoparticle	shell	*N*	*R* (Å)	ΔE_o (eV)	R-factor
Au:Pd = 1:3 Sub:Cat = 250:1	Pd−Pd	7.0(0.2)	2.741(0.003)	−5.2(0.3)	0.003
	Pd−Au	2.7(0.3)	2.75(0.02)		
Au:Pd = 1:3 Pd:Sub = 1:1	Pd−Pd	6.8(0.2)	2.748(0.003)	−3.9(0.3)	0.003
	Pd−Au	2.8(0.3)	2.77(0.02)		
Au:Pd = 1:1 Pd:Sub = 1:1/2	Pd−Pd	4.9(0.2)	2.755(0.004)	−3.1(0.3)	0.006
	Pd−Au	4.8(0.4)	2.76(0.01)		
1:3 AuPd Coreshell	Pd−Pd	4.3(0.3)	2.75(0.01)	−4.5(0.6)	0.025
	Pd−Au	3.2(0.6)	2.79(0.01)		
	Au−Au	8.2(0.7)	2.84(0.01)	6.2(0.6)	
	Au−Pd	2.4(0.3)	2.79(0.01)		
Pd NPs	Pd−Pd	7.8(0.3)	2.740(0.005)	−4.8(0.4)	0.017
Au NPs	Au−Au	9.2(1.6)	2.83(0.01)	4.6(1.3)	0.029

[a]The σ^2 (Å^2) values for the Pd−Pd, Pd−Au (and Au−Pd), and Au−Au shells were fixed at 0.0079, 0.009, and 0.012 respectively. S_o^2 values of 0.93 and 0.91, determined from Pd and Au foils, were used for Pd and Au fitting, respectively.

had enhanced selectivities compared to those formed in situ.[24] Others have shown that AuPd catalysts form from monometallic Au and Pd nanoparticles and seem to be the active catalyst for the oxidation reaction.[33] It is not clear at this time why the behavior of pure Pd nanoparticles seems to differ from the AuPd system in terms of the active catalyst species for allylic alcohol oxidation; one point to mention is the Pd surfaces in this AuPd system are significantly 4d-electron poor (Figure 2), and can activate oxygen without actual PdO formation on the surface.

3.6. EXAFS Fitting and Structural Analysis of AuPd Nanoparticles. EXAFS structural analysis was performed on solution-phase NPs formed at the end of three different in situ liquid reactions at the Pd K edge. The Pd−K-edge EXAFS of solutions of presynthesized 1:3 sequentially reduced AuPd NPs and monometallic Pd NPs were also analyzed. Models for the 1:1 and 1:3 Au:Pd NPs were prepared based on weighted values of pure Au and Pd fcc structures, and the EXAFS data was fit to the model in R-space. Quality fits for all the samples were obtained, with the fits for the AuPd NPs formed in situ shown in Figure 6. A summary of the data determined by EXAFS fitting is given in Table 4. Because of time constraints it was not possible to collect Au L_{III} edge data after each in situ measurement; thus only Pd edge data was fit for in situ samples. The monometallic Pd and Au "core" NPs synthesized have a first shell coordination numbers of 7.8 and 9.2, respectively. Disorder parameters for all samples showed significant disorder in all bonds; this is likely due to both static and thermal

dx.doi.org/10.1021/cs400230t | ACS Catal. 2013, 3, 1411−1419

disorder, but no attempt was made to distinguish between these. Pd−Au bond lengths for most samples fell between Pd−Pd and Au−Au bond lengths, which is consistent with previous work in both our group and by others.[24,64,65]

For all three in situ reactions, it is also apparent from EXAFS analyses that the Pd(II) reduction is complete as no significant Pd−Cl or Pd−O contributions were seen in the final spectra. In the bulk material, a coordination number of 12 would be expected for a material composed of Pd and Au metals. Because NPs exhibit such a high degree of surface area, many surface atoms are left without neighboring atoms. Therefore, a coordination number less than 12 is expected for the NPs analyzed. For each spectrum, the Pd−Pd and Pd−Au coordination numbers were obtained ((N_{Pd-Pd}) and (N_{Pd-Au}), respectively). For the two in situ reactions performed at a Au NP:Pd(II) ratio of 1:3 there is no significant difference in coordination numbers. Finally, the NPs formed with an Au:Pd ratio of 1:1 have lower Pd−Pd and higher Pd−Au coordination numbers than the 1:3 AuPd NPs. With less Pd in the system it would be expected that a thinner shell of Pd can be reduced onto the Au NP surface. The smaller Pd−Pd coordination number of the 1:1 NPs suggests that there are more surface Pd atoms in this system than in the 1:3 AuPd system, but the larger Pd−Au coordination number suggests that more Au−Pd mixing is also seen in this sample. The Pd−Pd first shell coordination numbers in all the samples are significantly below that of pure Pd NPs (particularly for the 1:1 Au:Pd ratio; while it is possible that there may be some secondary nucleation of Pd NPs in the system, it is apparent from EXAFS data that most of the Pd is deposited on existing Au nanoparticles in the solution. However, given that only Pd K edge data was obtained on most samples, and given the large polydispersities of AuPd nanoparticles generated at the high concentrations necessary for in situ XAS measurements (typically ~6.0 ± 3.0 nm), there is likely to be some structural inhomogeneities. EXAFS data does, however, definitively show complete reduction of the Pd with no significant Pd−O or Pd−Cl contributions. In addition, in situ Pd L_{III} edge data (Figures 2 and 5) does support that Pd is depositing onto the Au given the appearance of a slightly increased white line intensity after reduction and the unreactivity of the final particles toward oxidation.

Finally, a comparison was made between the in situ formed AuPd nanoparticles analyzed and sequentially formed 1:3 Au:Pd NPs synthesized ex situ using an ascorbic acid secondary reductant. A lower N_{total} value for Pd of 7.5 was seen for the sequentially formed particles via ascorbic acid reduction compared to the AuPd particles made in situ via crotyl alcohol reduction. This indicates that NPs made by the controlled reduction of Pd onto Au seeds by ascorbic acid produced particles with significantly Pd rich surfaces. However, the higher degree of Pd−Au bonding in these same particles suggests that these NPs have some AuPd mixing, which potentially is an aging effect (the ascorbic acid nanoparticles were made approximately one week before analysis). We are planning to more thoroughly examine the effect of aging on nanoparticle structure in future studies.

4. CONCLUSIONS

We have shown that quick scan, in situ X-ray absorption spectroscopic experiments can yield valuable information on nanoparticle-catalyzed reactions in solution. The AuPd nanoparticle-catalyzed oxidation of crotyl alcohol in water was studied by in situ XAS analysis. It was found that, when using Au(0) nanoparticles in the presence of Pd(II) as the reaction catalyst, the Pd(II) becomes reduced to Pd(0) upon exposure to the crotyl alcohol. In addition, the products from this reaction (in situ formed AuPd NPs) were treated with O_2 for up to 3 h, and no significant changes in the spectra or coordination numbers were seen. This suggests that the Pd on the surface of the Au nanoparticles is quite stable to oxidation under these conditions.

AUTHOR INFORMATION

Corresponding Author

*E-mail: robert.scott@usask.ca. Phone: 306-966-2017. Fax: 306-966-4730.

Notes

The authors declare no competing financial interest.

ACKNOWLEDGMENTS

The authors would like to thank NSERC and the University of Saskatchewan for funding. The authors would also like to thank Drs. Tianpin Wu, Jeremy Kropf, and Trudy Bolin at the Advanced Photon Source (APS) for the assistance with EXAFS and XANES measurements. Use of the Advanced Photon Source is also supported by the U.S. Department of Energy, Office of Science, Office of Basic Energy Sciences, under Contract DE-AC02-06CH11357. PNC/XOR facilities at the Advanced Photon Source, and research at these facilities, are supported by the U.S. Department of Energy-Basic Energy Sciences, a Major Resources Support grant from NSERC, the University of Washington, Simon Fraser University, and the Advanced Photon Source. MRCAT operations are supported by the Department of Energy and the MRCAT member institutions. Funding for J.T.M. is based upon work supported as part of the Institute for Atom-efficient Chemical Transformations (IACT), an Energy Frontier Research Center funded by the U.S. Department of Energy, Office of Science, Office of Basic Energy Sciences.

REFERENCES

(1) Haruta, M.; Yamada, Y.; Kobayashi, T.; Iijima, S. *J. Catal.* **1989**, *115*, 301−309.
(2) Haruta, M. *Catal. Today* **1997**, *36*, 153−166.
(3) Tsunoyama, H.; Sakurai, H.; Negishi, Y.; Tsukuda, T. *J. Am. Chem. Soc.* **2005**, *127*, 9374−9375.
(4) Dimitratos, N.; Lopez-Sanches, J. A.; Lennon, D.; Porta, F.; Prati, L.; Villa, A. *Catal. Lett.* **2006**, *108*, 147−153.
(5) Kanaoka, S.; Yagi, N.; Fukuyama, Y.; Aoshima, S.; Tsunoyama, H.; Tsukuda, T.; Sakurai, H. *J. Am. Chem. Soc.* **2007**, *129*, 12060−12061.
(6) Dimitratos, N.; Lopez-Sanches, J. A.; Anthonykutty, J. M.; Brett, G.; Carley, A. F.; Tiruvalam, R. C.; Herzing, A. A.; Kiely, C. J.; Knight, D. W.; Hutchings, G. J. *Phys. Chem. Chem. Phys.* **2009**, 4952−4961.
(7) Enache, D. I.; Knight, D. W.; Hutchings, G. J. *Catal. Lett.* **2005**, 103.
(8) Abad, A.; Almela, C.; Corma, A.; Garcia, H. *Chem. Commun.* **2006**, 3178−3180.
(9) Miedziak, P.; Sankar, M.; Dimitratos, N.; Lopez-Sanches, J. A.; Carley, A. F.; Knight, D. W.; Taylor, S. H.; Kiely, C. J.; Hutchings, G. J. *Catal. Today* **2011**, *164*, 315−319.
(10) Evangelisi, C.; Schiavi, E.; Aronica, L. A.; Caporusso, A. M.; Vitulli, G.; Bertinetti, L.; Martra, G.; Balerna, A.; Mobilio, S. *J. Catal.* **2012**, *286*, 224−236.
(11) Mallin, M. P.; Murphy, C. J. *Nano Lett.* **2002**, *2*, 1235−1237.
(12) Kim, M.; Na, H.; Lee, K. C.; Yoo, E. A.; Lee, M. *J. Mater. Chem.* **2003**, *13*, 1789−1792.

(13) Agrawal, V. V.; Mahalakshmi, P.; Kulkarni, G. U.; Rao, C. N. R. *Langmuir* **2005**, *22*, 1846−1851.
(14) Lee, W.; Kim, M. G.; Choi, J.; Park, J.; Ko, S. J.; Oh, S. J.; Cheon, J. *J. Am. Chem. Soc.* **2005**, *127*, 16090−16097.
(15) Rapallo, R.; Rossi, G.; Ferrando, R.; Fortunelli, A.; Curley, B. C.; Lloyd, L. D.; Tarbuck, G. M.; Johnston, R. L. *J. Chem. Phys.* **2005**, *122*, 194308.
(16) Dimitratos, N.; Villa, A.; Wang, D.; Porta, F.; Su, D.; Prati, L. *J. Catal.* **2006**, *244*, 113−121.
(17) Enache, E. I.; Edwards, J. K.; Landon, P.; Solsona-Espriu, B.; Carley, A. F.; Herzing, A. A.; Watanabe, M.; Kiely, C. J.; Knight, D. W.; Hutchings, G. J. *Science* **2006**, *311*, 362−365.
(18) Chaki, N. K.; Tsunoyama, H.; Negishi, Y.; Sakurai, H.; Tsukuda, T. *J. Phys. Chem. C* **2007**, *111*, 4885−4888.
(19) Liu, X.; Wang, A.; Wang, X.; Mou, C.; Zhang, T. *Chem. Commun.* **2008**, 3187−3189.
(20) Bracey, C. L.; Ellis, P. R.; Hutchings, G. J. *Chem. Soc. Rev.* **2009**, *38*, 2231−2243.
(21) Tsuji, M.; Matsunaga, M.; Ishizaki, T.; Nonaka, T. *CrystEngComm* **2012**, *14*, 3623−3632.
(22) Caron, S.; Dugger, R. W.; Ruggeri, S. G.; Ragan, J. A.; Ripin, D. H. B. *Chem. Rev.* **2006**, 2943−2989.
(23) Hou, W.; Dehm, N. A.; Scott, R. W. J. *J. Catal.* **2008**, *253*, 22−27.
(24) Balcha, T.; Strobl, J. R.; Fowler, C.; Dash, P.; Scott, R. W. J. *ACS Catal.* **2011**, *1*, 425−436.
(25) Carrettin, S.; McMorn, P.; Johnston, P.; Griffin, K.; Hutchings, G. J. *Chem. Commun.* **2002**, 696−697.
(26) Kon, Y.; Usui, Y.; Sato, K. *Chem. Commun.* **2007**, 4399−4400.
(27) Lee, A. F.; Hackett, S. F. J.; Hutchings, G. J.; Lizzit, S.; Naughton, J.; Wilson, K. *Catal. Today* **2009**, *145*, 251−257.
(28) Villa, A.; Janjic, N.; Spontoni, P.; Wang, D.; Su, D. S.; Prati, L. *Appl. Catal., A* **2009**, *364*, 221−228.
(29) Frank, A. J.; Rawski, J.; Maly, K. E.; Kitaev, V. *Green Chem.* **2010**, *12*, 1615−1622.
(30) Lee, A. F.; Ellis, C. V.; Wilson, K.; Hondow, N. S. *Catal. Today* **2010**, *157*, 243−249.
(31) Naughton, J.; Lee, A. F.; Thompson, S.; Vinod, C. P.; Wilson, K. *Phys. Chem. Chem. Phys.* **2010**, *12*, 2670−2678.
(32) Villa, A.; Wang, D.; Spontoni, P.; Arrigo, R.; Su, D.; Prati, L. *Catal. Today* **2010**, *157*, 89−93.
(33) Wang, D.; Villa, A.; Spontoni, P.; Su, D.; Prati, L. *Chem.—Eur. J.* **2010**, *16*, 10007−10013.
(34) Lee, A. F.; Ellis, C. V.; Naughton, J. N.; Newton, M. A.; Parlett, C. M. A.; Wilson, K. *J. Am. Chem. Soc.* **2011**, *133*, 5724−5727.
(35) Prati, L.; Villa, A.; Chan-Thaw, C. E.; Arrigo, R.; Wang, D.; Su, D. S. *Faraday Discuss.* **2011**, *152*, 353−365.
(36) Sankar, M.; Nowicka, E.; Tiruvalam, R.; He, Q.; Taylor, S. H.; Kiely, C. J.; Bethell, D.; Knight, D. W.; Hutchings, G. J. *Chem.—Eur. J.* **2011**, *17*, 6524−6532.
(37) Alhumaimess, M.; Lin, Z.; Weng, W.; Dimitratos, N.; Dummer, N. F.; Taylor, S. H.; Bartley, J. K.; Kiely, C. J.; Hutchings, G. J. *ChemSusChem* **2012**, *5*, 125−131.
(38) Dimitratos, N.; Lopez-Sanchez, J. A.; Hutchings, G. J. *Chem. Sci.* **2012**, *3*, 20−44.
(39) Keresszegi, C.; Ferri, D.; Mallat, T.; Baiker, A. *J. Phys. Chem. B* **2005**, *109*, 958−967.
(40) Lee, A. F.; Wilson, K. *Green Chem.* **2004**, *6*, 37−42.
(41) Meitzner, G.; Via, G. H.; Lytle, F. W.; Sinfelt, J. H. *J. Chem. Phys.* **1985**, *83*, 4793−4799.
(42) Toshima, N.; Harada, M.; Yonezawa, T.; Kushihashi, K.; Asakura, K. *J. Phys. Chem.* **1991**, *95*, 7448−7453.
(43) Hwang, B.; Sarma, L. S.; Chen, J.; Chen, C.; Shih, S.; Wang, G.; Liu, D.; Lee, J.; Tang, M. *J. Am. Chem. Soc.* **2005**, *127*, 11140−11145.
(44) Mikhlin, Y.; Likhatski, M.; Tomashevich, Y.; Romanchenko, A.; Erenburg, S.; Trubina, S. *J. Electron Spectrosc. Relat. Phenom.* **2010**, *177*, 24−29.
(45) Liu, F.; Zhang, P. *Appl. Phys. Lett.* **2010**, *96*, 043105.
(46) Nelson, R. C.; Miller, J. T. *Catal. Sci. Technol.* **2011**, *2*, 461−470.
(47) Imai, H.; Izumi, K.; Matsumoto, M.; Kubo, Y.; Kato, K.; Imai, Y. *J. Am. Chem. Soc.* **2009**, *131*, 6293−6300.
(48) Imai, H.; Matsumoto, M.; Miyazaki, T.; Kato, K.; Tanida, H.; Uruga, T. *Chem. Commun.* **2011**, *47*, 3538−3540.
(49) Ishiguro, N.; Saida, T.; Uruga, T.; Nagamatsu, S.-i.; Sekizawa, O.; Nitta, K.; Yamamoto, T.; Ohkoshi, S.-i.; Iwasawa, Y.; Yokoyama, T.; Tada, M. *ACS Catal.* **2012**, *2*, 1319−1330.
(50) Dash, P.; Bond, T.; Fowler, C.; Hou, W.; Coombs, N.; Scott, R. W. J. *J. Phys. Chem. C* **2009**, *113*, 12719−12730.
(51) Abramoff, M. D.; Magalhaes, P. J.; Ram, S. J. *Biophotonics Int.* **2004**, *11*, 36−42.
(52) Newville, M. *J. Synchrotron Radiat.* **2001**, *8*, 322−324.
(53) Ravel, B. *J. Synchrotron Radiat.* **2001**, *8*, 314−316.
(54) Ravel, B.; Newville, M. *J. Synchrotron Radiat.* **2005**, *12*, 537−541.
(55) Maeland, A.; Flanagan, T. B. *Can. J. Phys.* **1964**, *42*, 2364−2366.
(56) Meitzner, G.; Sinfelt, J. H. *Catal. Lett.* **1995**, *30*, 1−10.
(57) Huang, D. C.; Chang, K. H.; Pong, W. F.; Tseng, P. K.; Hung, K. J.; Huang, W. F. *Catal. Lett.* **1998**, *53*, 155−159.
(58) Sham, T. K.; Naftel, S. J.; Coulthard, I. *J. Appl. Phys.* **1996**, *79*, 7134−7138.
(59) Pearson, D. H.; Ahn, C. C.; Fultz, B. *Phys. Rev. B* **1993**, *47*, 8471−8478.
(60) Tsuji, J.; Nagashima, H.; Hori, K. *Chem. Lett.* **1980**, 257−260.
(61) Zaw, K.; Lautens, M.; Henry, P. M. *Organometallics* **1983**, *2*, 197−199.
(62) Scott, R. W. J.; Ye, H.; Henriquez, R. R.; Crooks, R. M. *Chem. Mater.* **2003**, *15*, 3873−3878.
(63) Gao, F.; Wang, Y.; Goodman, D. W. *J. Phys. Chem. C* **2009**, *113*, 14993−15000.
(64) Liu, F.; Wechsler, D.; Zhang, P. *Chem. Phys. Lett.* **2008**, *461*, 254−259.
(65) Fang, Y.-L.; Miller, J. T.; Guo, N.; Heck, K. N.; Alvarez, P. J. J.; Wong, M. S. *Catal. Today* **2011**, *160*, 96−102.